Probing the dynamics of cell differentiation in a model of *Drosophila* neurogenesis

George Marnellos
Sloan Center for Theoretical Neurobiology,
The Salk Institute, La Jolla, CA 92037, USA

Eric Mjolsness
Machine Learning Systems Group,
Jet Propulsion Laboratory,
Pasadena, CA 91109, USA

Abstract

We have formulated a computational model of *Drosophila* early neurogenesis, the process by which neuroblasts and sensory organ precursor (SOP) cells differentiate from within proneural clusters of cells. The model includes intracellular gene regulatory interactions as well as lateral cell-cell signalling. It makes predictions about how the interplay of factors like proneural cluster shape and size, gene expression levels, and strength of cell-cell signalling determines the timing and position of appearance of neuroblasts and SOP cells; and about the robustness of this process and the effects of gene product level perturbations on cell differentiation.

Introduction

One of the very early steps in neural development is the generation of neuronal precursor cells in appropriate numbers and their precise positioning, which to a large extent determines the identity of their progeny. In *Drosophila*, neuroblasts and sensory organ precursor (SOP) cells differentiate from epithelia to give rise to the central nervous system in the fly embryo and to epidermal sensory organs in the peripheral nervous system of the adult fly, respectively. Neuroblasts are precursor cells that divide to form neurons and glia; they segregate from the ventral neuroectoderm of the embryo in a regular segmental pattern (Bate 1976). SOPs appear at stereotypical positions on imaginal discs (which are primordia giving rise to appendages like wings, legs, eyes and antennae) during late larval and early pupal stages and divide to produce a neuron and three other cells that form *Drosophila*'s sensory organs, like the bristles on its thorax (Hartenstein & Posakony 1989).

The activities of two main sets of genes working in opposite directions are thought to underlie this differentiation process: one promoting neural development and the other preventing it and favoring epidermal development. Cell-cell signalling is believed to be an essential part of this specification of cell fate and thus *Drosophila* neurogenesis is an example of many such related processes of cell differentiation in epithelia both in invertebrate and vertebrate organisms — see recent reviews (Campuzano & Modollel 1992; Muskavitch 1994; Artavanis-Tsakonas, Matsuno, & Fortini 1995).

More specifically, neuroblasts and SOPs differentiate from clusters of apparently equivalent cells which at some stage all have the potential to adopt the neural fate (Stern 1954), as ablation studies have shown (Doe & Goodman 1985a; 1985b). These cell clusters express genes of the *achaete-scute* complex, so called *proneural* genes, which all encode transcription activators and confer to cluster cells the potential to adopt the neural fate (Romani *et al.* 1989; Cubas *et al.* 1991; Skeath & Carroll 1991; 1992); the clusters are therefore called proneural clusters (see Fig. 1).

The other set of genes involved in neurogenesis includes a number of genes also encoding nuclear proteins, for instance genes of the *Enhancer-of-split* (*E(spl)*) complex and *hairy*, as well as other genes for membrane and cytoplasmic proteins; all these tend to suppress neurogenesis and promote epidermal development. In this paper we refer to this set of genes as *epithelial* genes — in the literature they are called "neurogenic" genes, because loss-of-function mutations of these genes lead to overproduction of neurons (Poulson 1940; Lehmann *et al.* 1983; Skeath & Carroll 1992), but we have avoided this term as it might create confusion with proneural genes.

Expression of proneural genes in embryonic neuroectoderm and imaginal disc clusters eventually gets restricted to a single cell per cluster, in the case of the neuroectoderm, or very few cells per cluster, in the case of imaginal discs (clusters in the discs are typically larger than those in the neuroectoderm); in these cells, the future neuroblasts or SOPs, proneural expression increases, whereas in the remaining cluster cells it ceases and those cells become epidermal (Cubas *et al.* 1991; Martin-Bermudo *et al.* 1991; Skeath & Carroll 1991; 1992); the whole process is referred to as "cluster resolution". Cluster resolution and the singling out of neural precursors from within proneural clusters is brought

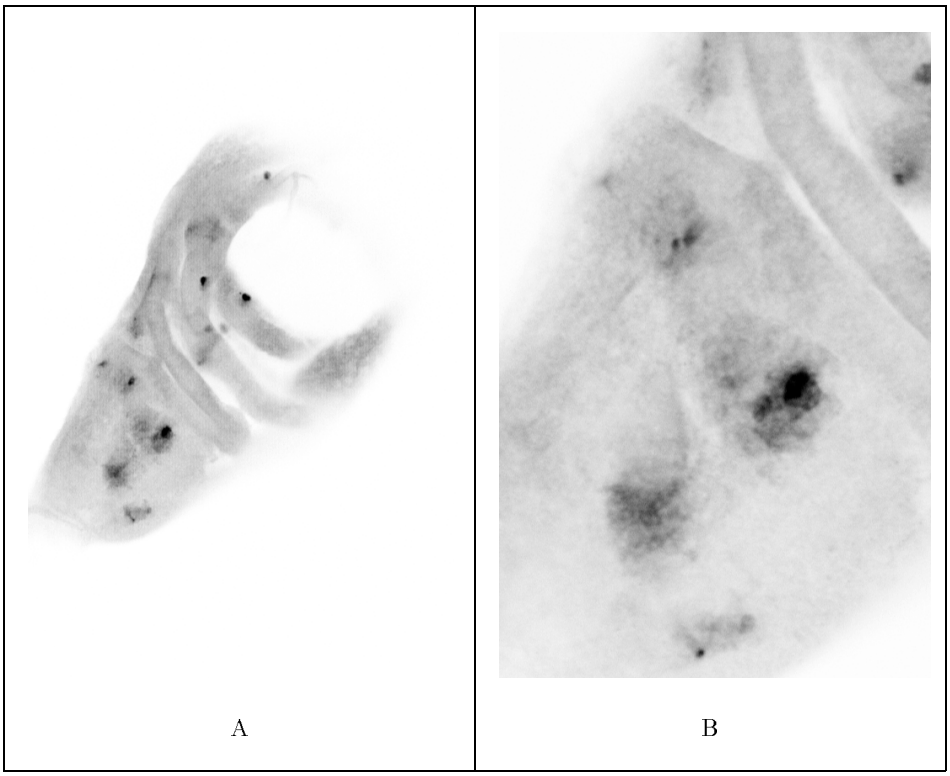

Figure 1: (A) Proneural gene expression in clusters in a *Drosophila* wing disc (the appendage of the fly larva that gives rise to the wing and the back of the adult). The *lacZ* reporter indicates *achaete* expression (*achaete* is one of the proneural genes). (B) Detail of (A), note cluster on lower left that has not yet resolved; other clusters appear to be at a more advanced stage of resolution. We have used the enhancer-trap line A1-1, which expresses the reporter *lacZ* gene under the influence of *cis*-elements in the promoter of *achaete* (van Doren *et al.* 1992); we have stained with anti β-gal antibody and secondary fluorescent antibody; images were obtained with a Bio-Rad MRC1000UV confocal microscope and processed with the NIH-Image program.

about by inhibitory lateral signalling between adjacent cells, through which the neural fate is promoted in the future neuroblasts and SOPs and suppressed in other cells (Wigglesworth 1940; Stern 1954; Doe & Goodman 1985a; 1985b). The lateral signal is transmitted by the product of *Delta* which is a ligand of the receptor encoded by *Notch* (Fehon *et al.* 1990; Heitzler & Simpson 1991; Struhl, Fitzgerald, & Greenwald 1993). The signal is relayed from Notch to epithelial genes through a protein that has been shown to directly activate *E(spl)* transcription (Fortini & Artavanis-Tsakonas 1994; Jarriault *et al.* 1995; Bailey & Posakony 1995)

Despite the amount of experimental data that have been gathered, several features of the neural fate determination process remain unexplained. A precise characterization of the function of lateral signalling is still lacking. Some researchers have described the singling out of neural precursors from equivalence groups as a process in which one of the cells in the group receives an initial push to become a neural precursor, in an unspecified, perhaps stochastic, manner, and this cell then extinguishes the neural potential in the other cells of the proneural cluster through "lateral inhibition" (Wigglesworth 1940; Stern 1954), possibly amplifying its own inhibitory power and weakening that of its neighbors through a feedback mechanism (Heitzler & Simpson 1991). Other researchers have favored a scheme of "mutual inhibition", in which all cells in a proneural cluster, including the future neural precursor, are subject to inhibition by other cells in the cluster, but the future precursor has additional means to shield itself from inhibition (Goriely *et al.* 1991; Muskavitch 1994; Bang, Bailey, & Posakony 1995). There are also questions about how important interactions of range longer than that of lateral signalling are: it is not clear, for instance, how crucial diffusible factors are for the resolution of proneural clusters.

Dynamical aspects of cluster resolution are poorly understood. It is not known, for example, whether and how the shape and size of proneural clusters can determine how cluster resolution proceeds: although there have been some observations regarding shapes of clusters, and descriptions of subsets of cells (often centrally located) in the clusters from which future neural pre-

cursors are more likely to emerge (Goriely *et al.* 1991; Cubas *et al.* 1991) as well as some work on the temporal sequence of neural precursor emergence (Huang, Dambly-Chaudière, & Ghysen 1991), there has been no systematic study of how shape or size of clusters might affect the position and timing of neural precursor emergence.

In order to address questions like these and investigate the interplay between proneural and epithelial genes and the genes that mediate cell-cell signalling, we have constructed a model which is presented below; it is an extension of a model that was first described in Marnellos (1997).

Model

In our model, cells are represented as overlapping circles in a 2-dimensional hexagonal lattice; the extent of overlap determines the strength of interaction between neighboring cells (see Fig. 2). Cells in the model express a small number of genes corresponding to genes that are involved in neuroblast and SOP differentiation. In the work presented here we have used networks with four genes (one corresponding to the proneural group, another for the epithelial group and two for the ligand and receptor, respectively, mediating cell-cell signalling). The model has been based on a framework introduced in Mjolsness *et al.* (1991) to simulate developmental processes through the use of regulatory gene networks; a framework very similar to this in scope and structure, but with some differences in how state changes in cells are represented, has also been proposed by Fleischer and Barr (Fleischer & Barr 1994; Fleischer 1995).

Genes interact as nodes in recurrent neural nets: A gene a sums inputs from genes in the same cell or in neighboring cells at time t according to the following equation

$$u_a(t) = \sum_b T_{ab} v_b(t) \tag{1}$$

where T is the matrix of gene interactions and $v_b(t)$ gene product concentrations within the cell; the T matrix has the structure depicted in the table below; columns in this table are for input genes and rows for genes affected (empty boxes signify zero interaction strength. i.e. no interaction):

Intracellular Interactions				
	Proneural	Epithelial	Receptor	Ligand
Proneural	♦	♦		
Epithelial	♦	♦		
Receptor	♦	♦		
Ligand	♦	♦		

This table shows that we have allowed only proneural and epithelial gene products to directly regulate the expression of other genes (themselves included), since these two genes correspond to transcription factors in the real biological system.

Concentration $v_a(t)$ of the product of gene a then changes according to

$$\frac{dv_a}{dt} = R_a g(u_a(t) + h_a) - \lambda_a v_a(t) \tag{2}$$

where $u_a(t)$ is the linear sum of Eq. 1, g a sigmoid function, R_a the rate of production of gene a's product, h_a the threshold of activation of gene a and λ_a the rate of decay of gene a product. We integrate these differential equations using Euler's method (we use 150 time steps).

We have modeled lateral interactions between cells by the binding of ligand to the receptor in the neighboring cell and subsequent regulation of the epithelial gene by the active ligand-receptor complex — this corresponds to the signal relayed from activated Notch receptor to epithelial gene *E(spl)*, as was mentioned in the Introduction. In more detail, the ligand-receptor reaction is taken to be of the following form:

$$L + R \leftrightarrows L \circ R \tag{3}$$

where L is ligand (on one cell), R receptor (on a neighboring cell) and $L \circ R$ the active receptor-ligand complex; the rate of the reaction to the right is k_1 and to the left k_2. If v_L is ligand concentration, v_R receptor concentration and $[L \circ R]$ concentration of the receptor-ligand active complex, we have that

$$\frac{d[L \circ R]}{dt} = k_1 v_L v_R - k_2 [L \circ R] \tag{4}$$

$$\frac{dv_L}{dt} = \frac{dv_R}{dt} = -k_1 v_L v_R + k_2 [L \circ R]. \tag{5}$$

This reaction is assumed to take place at a much faster timescale than gene expression and to have reached a steady state before influencing gene expression. From Eqs. 4 and 5, at this steady state we have

$$[L \circ R] = k v_L v_R \tag{6}$$

where $k = \frac{k_1}{k_2}$. Thus the epithelial gene in a cell receives input from receptor-ligand complexes activated by ligand in the six surrounding cells (the lattice is hexagonal); this can be represented as an extra term $\hat{u}_E$ that is added to u_E (which is the sum of inputs u for the epithelial gene, see Eq. 1) before Eq. 2 is calculated

$$\hat{u}_E = \sum_{i \in N} \Lambda^i \hat{T}_E [L \circ R]^i \tag{7}$$

where N is the set of six surrounding cells, Λ^i a factor depending on the overlap of the cell with neighboring cell i (as measured for instance by the common chord of the two circles), $\hat{T}_E$ the strength of the action of the receptor-ligand complex on the epithelial gene (k of Eq. 6 has been included in $\hat{T}_E$), and finally $[L \circ R]^i$ is the concentration of receptor-ligand complex due to ligand on cell i. Because of Eq. 6, we can write this as

$$\hat{u}_E = \sum_{i \in N} \Lambda^i \hat{T}_E v_L^i v_R \quad (8)$$

where v_L^i is ligand concentration in neighboring cell i.

We optimize on gene interaction strengths, i.e. $\hat{T}_E$ of Eq. 7 and the eight T's of Eq. 1 (the other parameters in the equations above are kept constant) in order to fit gene expression patterns described in the literature; the cost function optimized is

$$E = \sum_{cells,genes,times} (v^i_{aMODEL}(t) - v^i_{aDATA}(t))^2, \quad (9)$$

which is the squared difference between gene product concentrations in the model and those in the dataset, summed over all cells and over all gene products and times for which data is available. We have used a stochastic algorithm, simulated annealing, for this optimization. For more details on the model and the optimization method used see Marnellos (1997).

Simulation Results

Design of optimization and test runs. The gene expression datasets we optimize on, the *training* datasets, are adapted from schematic results described in the experimental literature (Cubas *et al.* 1991; Skeath & Carroll 1992; Jennings *et al.* 1994); they specify the initial pattern of concentrations of gene products (i.e. the proneural clusters), the desired intermediate pattern, and the desired final pattern when the proneural clusters have resolved to single cells expressing the proneural gene at high levels (see Fig. 2); it is left to the optimization to find the right model parameters so that the system develops from the initial state through the intermediate one to the desired final one. The initial concentrations of receptor and ligand are uniform for all cells and their subsequent concentrations are not constrained by the dataset (in this respect, they are comparable to hidden units in neural nets).

All cells in a proneural cluster have initially the same gene expression levels. The size and cluster arrangement of the training datasets do not have any particular biological significance; the datasets have been designed in such a way as to keep the number of cells low while including as many clusters as possible, since optimization is very expensive computationally and so optimization runs on datasets with more cells than we have used would be impractical. We have used torus topology in our runs, although this does not appear to be a crucial factor in the results described here.

Robustness of solutions. We have tried to limit the number of parameters we optimize on (as was mentioned above, we optimize only on gene interaction strengths), in order to avoid overfitting our rather small datasets. The optimization procedure used (simulated annealing) has produced very good and consistent fits to the training datasets. For instance, out of the eight (8) good solutions obtained for the dataset in Fig. 2, six were very similar in their parameter values (same signs, similar orders of magnitude); so all these solutions probably come from the same optimum of the cost function, which may be one of very few large optima, or even the global optimum. Also, successful optimization runs have yielded solutions that not only perform well on the training dataset shown in Fig. 2 (see top row of Fig. 3) but also work for other datasets with clusters like those in the training dataset but with greater numbers of such clusters in various spatial arrangements (data not shown). This indicates that optimization does not just find parameter values that only work for the specific size and cluster arrangement of the training dataset, but rather produces solutions incorporating "rules" for cluster resolution.

In order to further evaluate these solutions and determine how robust they are and what they can tell us about the biological system under consideration, we have also run these solutions with different initial conditions, changes of solution parameter values, perturbations of gene expression during a run, as well as on *test* datasets containing novel, bigger or smaller, proneural clusters.

In Fig. 3, for instance, we have the same optimization solution parameters in both rows, but in the run of the top row initial concentrations of proneural and epithelial gene products are identical for all cells in a cluster, while in the bottom row initial proneural concentrations vary and differ between cells by about 10-15%. Despite this and despite the fact that, in this particular example, the future neural precursors start out with lower proneural concentrations than other cluster cells (even the lowest in the cluster), the pattern of cluster resolution remains identical as the end result shows (compare right panels of top and bottom rows of Fig. 3). So the optimization solutions are robust to small changes in initial conditions. Such robustness is a feature that a biological system would need during development.

Test datasets specify only initial concentrations and contain many more cells than training ones (since we do not optimize on them). An example appears in Fig. 4: it contains several clusters of various shapes and sizes, both

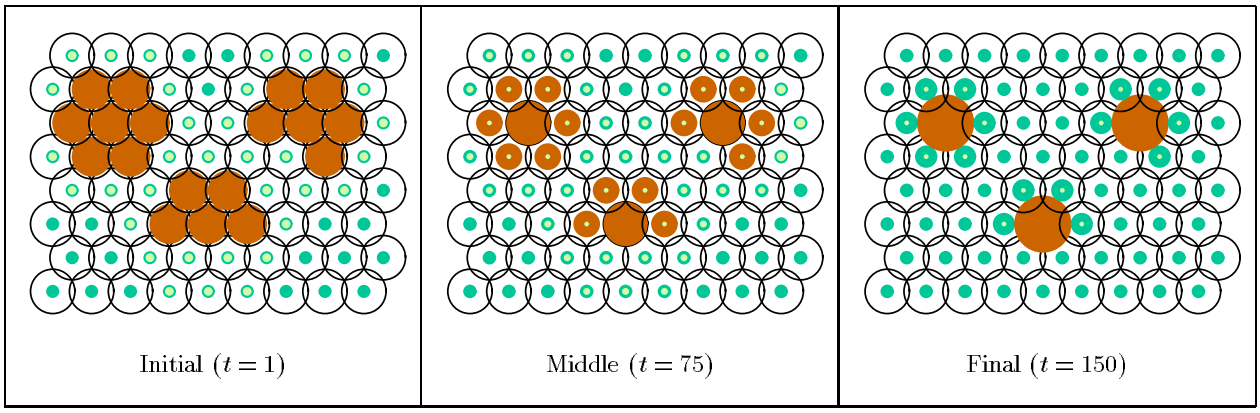

Figure 2: Cells are modeled as circles on a hexagonal lattice. Gene expression is represented by disks, proneural expression in brown, epithelial in green, and where the two overlap in yellow-green (dark, medium and light gray, respectively, in black-and-white); disk radius is proportional to level of expression. This figure shows the training dataset: on the left, the initial concentrations of the gene products — there is only proneural gene expression in three symmetrical clusters; in the middle, the desired intermediate pattern of expression; on the right, the desired final pattern of gene expression — proneural expression is retained only in the central cell of each cluster, the future neuroblast or SOP, whereas all other cells express the epithelial gene. Times (t) indicate the points in the run when the desired expression pattern is compared with the actual one (see Eq. 9); at $t = 1$ there is of course only initialization and no comparison. Initial concentrations of ligand and receptor are not shown.

smaller (4-cell clusters) and bigger (cluster in top right corner of panels in Fig. 4) than in the training dataset of Fig. 2. The test datasets could in principle have been used as training datasets, if it were not for the practical considerations mentioned above.

The optimization solution presented in Fig. 3 works well on the dataset of Fig. 4 too and resolves almost all clusters apart from the small, 4-cell ones; this is something we have observed in previous work with a model of similar structure to the one presented here and similar optimization procedures (Marnellos 1997; Marnellos & Mjolsness 1998): it is probably due to the fact that 4-cell clusters do not have a cell that is much more encircled than the others (as 5,6 and 7-cell of Fig. 4 do), but all cells are almost equally exposed. The optimization solution also resolves the big cluster in Fig. 4, for which it was not optimized; this is another aspect of the robustness of the solution.

Changes in initial proneural concentrations, as in the bottom row of Fig. 3, can be also studied in the dataset of Fig. 4 and usually do not alter the final outcome in the resolution of the big cluster, but in rare cases the big cluster does not resolve to a single cell but to two or three cells. This is consistent with experimental observations (Huang, Dambly-Chaudière, & Ghysen 1991) and provides an illustration of the interplay between position in cluster and level of proneural expression in determining whether a cell becomes a neural precursor or not.

A feature of our simulations that becomes apparent in Fig. 4 is that proneural expression in differentiated neural precursors decreases with time after they have been selected (see last panel, $t = 256$, in Fig. 4). This does not mean that the model diverges from biological observations at this point, but is simply a result of the fact that our model was not meant to deal with what happens after clusters resolve; in any case, in the actual biological system, neural precursors do not stay around expressing high levels of proneural proteins either, but, soon after they differentiate, they divide to give rise to neurons and glia and other cell types (Doe & Goodman 1985a; Hartenstein & Posakony 1989).

Dynamics of cluster resolution The parameters of the simulation in Fig. 4 are identical to those of the runs in Fig. 3, apart from one: the strength of lateral interactions through the receptor-ligand complex, i.e. $\hat{T}_E$ of Eqs. 7 and 8. Since lateral interactions are crucial for cluster resolution, we have varied their strength to see the effects on the dynamics of the whole process. In Fig. 4 the value of $\hat{T}_E$ is 25% higher than in Fig. 3; the stronger lateral interaction makes cluster resolution faster, as can be observed, for instance, when comparing the stage of resolution at $t = 76$ of the symmetrical, 7-cell clusters in Figs. 3 and 4: resolution has clearly progressed more in clusters of Fig. 4. The effect is much more pronounced for the big cluster of Fig. 4, which takes about 200 timesteps longer to resolve when lateral interaction strengths are 20-30% lower (not shown). At even higher values of $\hat{T}_E$, clusters start to fail to resolve and proneural expression is extinguished (not shown). When $\hat{T}_E = 0$, i.e. when lateral interactions are abolished, clusters do not resolve but all cells in them retain proneural gene expression. This parallels the effect of the

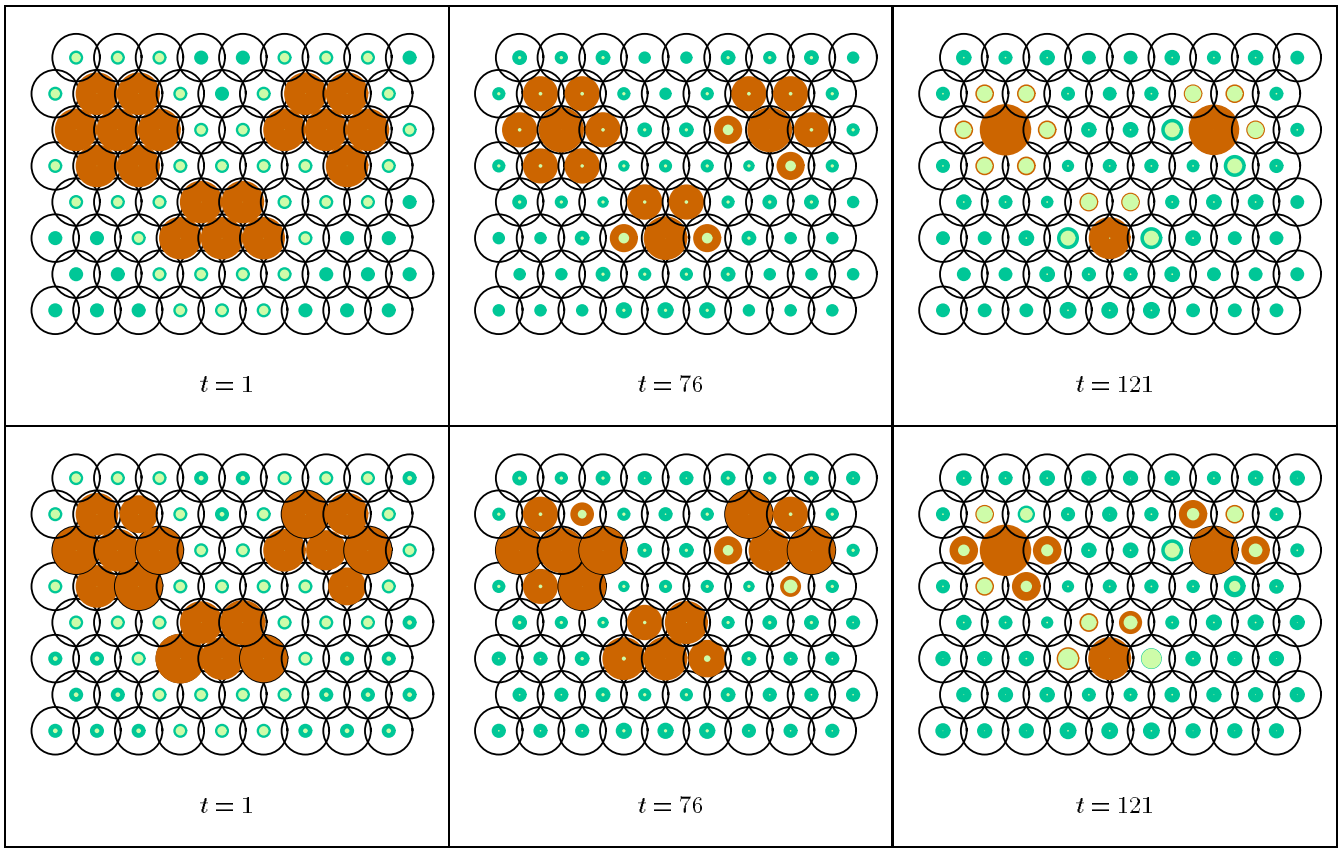

Figure 3: Computer simulation of neural precursor differentiation with parameter values in the model derived by optimization on the dataset of Fig. 2. From left to right, different time frames of the evolution of gene product concentrations. Top row: run with identical initial gene product concentrations for all cells in each proneural cluster. Bottom row: initial proneural concentrations vary by about 10-15% between cells in each cluster. In both runs the clusters resolve in the same way, as the comparison of the two panels at $t = 121$ shows (the only difference being that in the bottom run the clusters take slightly longer to resolve). This illustrates the robustness of cluster resolution to small changes in initial gene expression levels in proneural clusters. Conventions as in Fig. 2.

neurogenic mutations in the real biological system; these mutations disrupt lateral communication between cells and lead to overproduction of neurons (Poulson 1940; Lehmann *et al.* 1983; Skeath & Carroll 1992). Thus variation in the value of a single parameter, $\hat{T}_E$, can produce this "heterochronic" change in the process of cluster resolution or even prevent neural precursor differentiation. This is an interesting and testable prediction of the model.

The timing of cluster resolution also depends on the size of the cluster; bigger clusters take longer to resolve, which is something we have observed in previous work (Marnellos 1997; Marnellos & Mjolsness 1998), but which is much more evident in the example of Fig. 4.

To further probe the dynamics of cluster resolution, we have perturbed the levels of expression of proneural and epithelial genes in specific cells during a run, as illustrated in Fig. 5. In this simulation (which has the same initial concentrations as the one in Fig. 4 and uses the same parameter values, including $\hat{T}_E$) we instantaneously increased at $t = 60$ the level of epithelial expression in the central cell of a symmetrical, 7-cell cluster and also the level of proneural expression in a peripheral cell of a different symmetrical cluster. Whereas the first perturbation prevents normal resolution of the cluster involved, (as can be observed at $t = 121$ for instance), the second one has no effect on resolution and the cluster involved resolves normally (see Fig. 5). The effects of such perturbations will vary depending on the time and cell in which they are carried out, and on whether they occur singly, as in the two examples of Fig. 5, or in various combinations. Such manipulations are therefore a rich source of predictions of the model.

Discussion

In this paper we have extended and slightly modified a *Drosophila* neurogenesis model introduced in Marnellos (1997), in order to make it more biologically realistic. The previous model had only proneural and epithelial genes that could interact with each other across

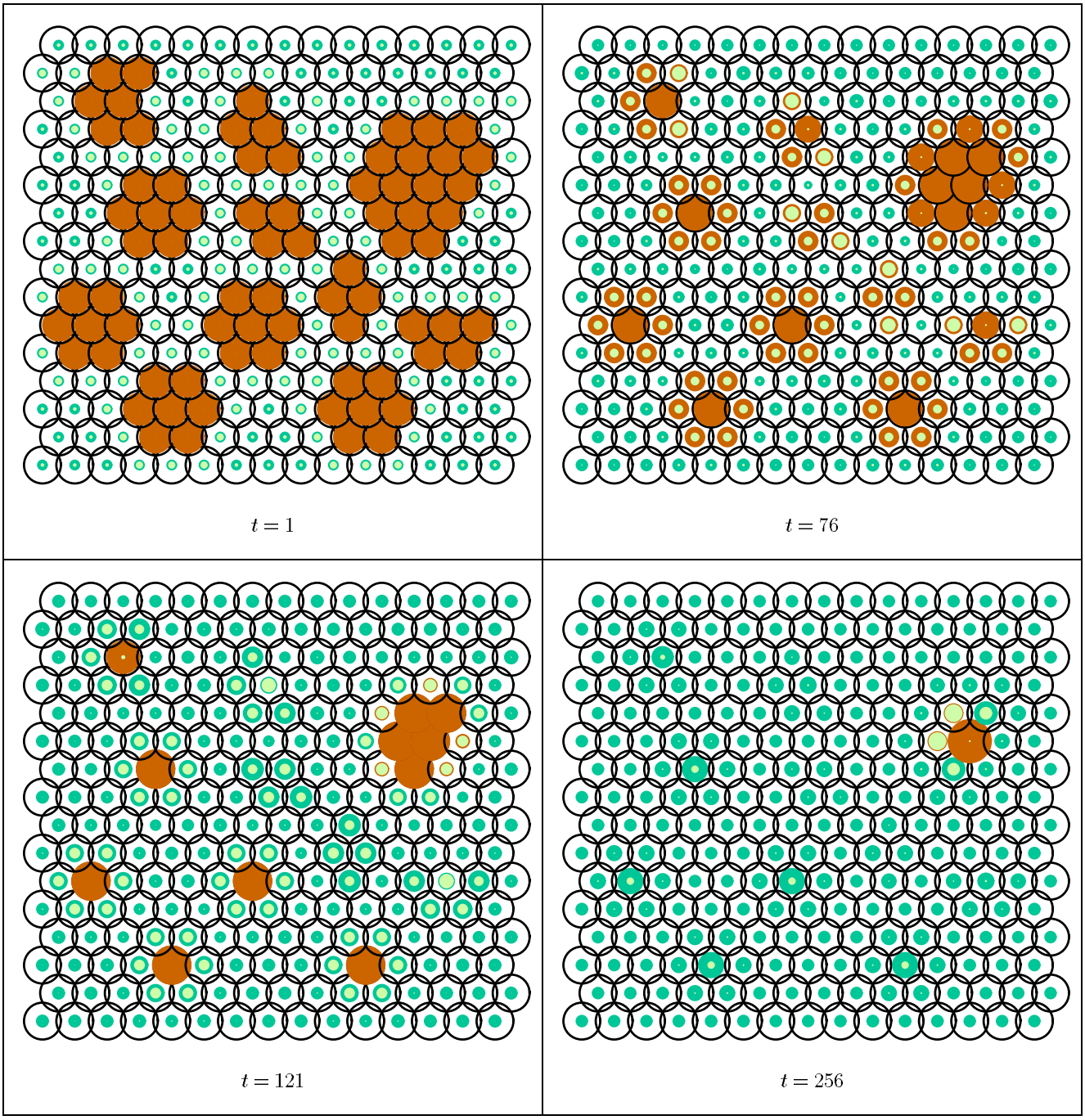

Figure 4: Simulation using a test dataset with clusters of various shapes and sizes. The parameter values are almost all identical to those of the simulations in Fig. 3. All clusters, except for the 4-cell ones, successfully resolve. The big cluster takes much longer than other clusters to resolve. The strength of the lateral interaction, $\hat{I}_E$ of Eqs. 7 and 8, is greater in this simulation than in those of Fig. 3. This has a "heterochronic" effect: it makes clusters resolve faster, as can be seen by comparing the degree of resolution of symmetrical, 7-cell clusters at $t = 76$ in this Figure with those of Fig. 3. Same conventions as in Fig. 2.

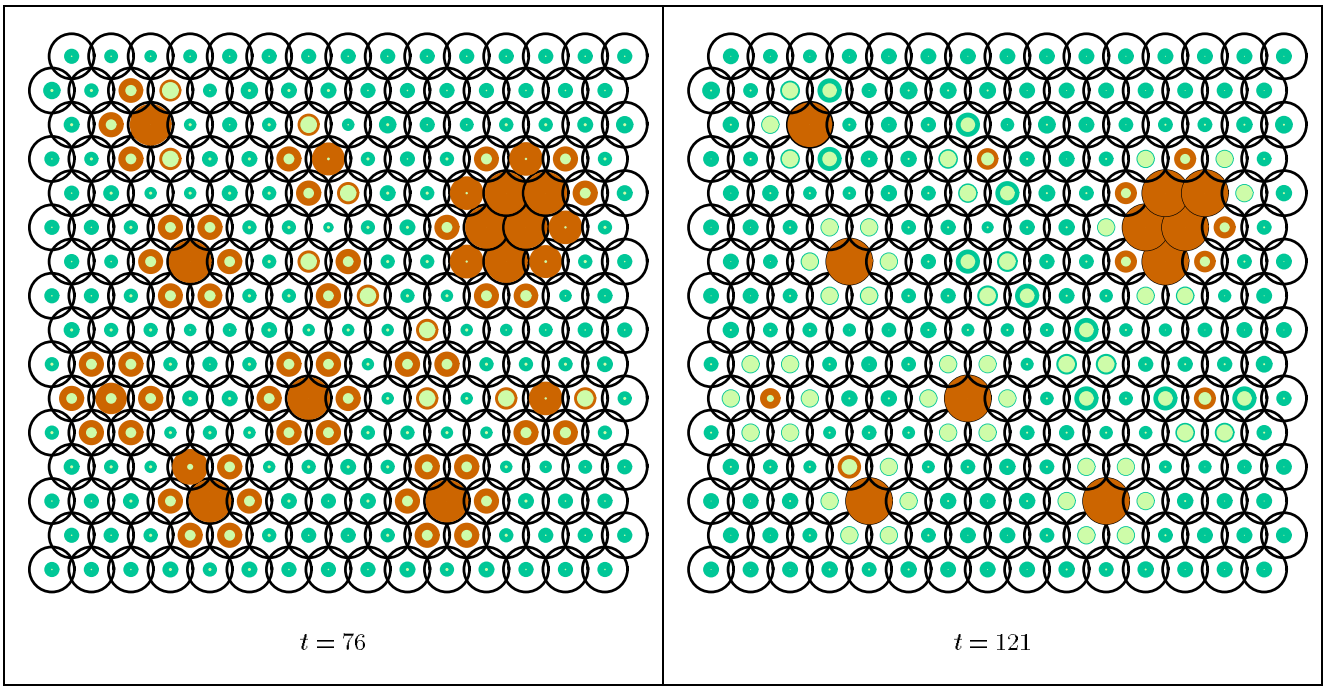

Figure 5: Simulation with perturbations of gene expression in individual cells of two symmetrical, 7-cell clusters. The clusters are the two ones in the lower left corner of the dataset. At $t = 60$ the level of epithelial expression in the central cell of the upper one of these two clusters was instantaneously increased, while in the lower cluster proneural expression was increased in a peripheral cell. Both perturbations can be detected in the left panel ($t = 76$). The first perturbation abolishes cluster resolution, while the second has no effect on resolution, as can be seen in the right panel (and also in comparison with the corresponding panel of Fig. 4).

cells; this afforded much greater flexibility in cell-cell signalling than has been experimentally observed in this system. In the work presented here we have included genes for a receptor and a ligand that gate communication across cells; such communication can now occur only through the interaction of an activated receptor-ligand complex with the epithelial gene, as has been described in the literature (Fortini & Artavanis-Tsakonas 1994; Jarriault *et al.* 1995; Bailey & Posakony 1995). The increase in the number of genes has been accomplished without an accompanying increase in the number of optimized parameters. The size of the training datasets has also increased with the addition of desired intermediate concentrations: performance is now scored in the middle and at the end of a run, instead of only at the end. This more constrained optimization has yielded many good and consistent solutions. The training datasets now have one 7-cell, one 6-cell and one 5-cell cluster, instead of only symmetrical 7-cell clusters, and this may have made the optimization solutions better at resolving novel types of clusters.

In the present model the strength of lateral signalling during a run is modulated by changes in receptor and ligand concentrations, whereas in the original model similar but less flexible modulation was afforded by the inclusion of cell delamination (absent here) which changed the area of contact between adjacent cells and contributed to the resolution of larger clusters. Although neuroblast delamination accompanies cluster resolution in the central nervous system of the *Drosophila* embryo, delamination does not occur during cluster resolution in imaginal discs and may not be necessary for resolution; the present model is therefore more consistent with experimental evidence.

Our results here have reconfirmed findings of the previous model (Marnellos 1997; Marnellos & Mjolsness 1998): for instance, that smaller clusters generally resolve faster than larger ones (Fig. 4); that lateral signalling is crucial for cluster resolution and when it is abolished clusters do not resolve (which parallels the neurogenic mutant phenotype in the biological system); or that cell-cell interactions involving just the immediate neighborhood of any given cell can bring about cluster resolution, without the need of other longer range processes like diffusion (even though the existence of such processes cannot be ruled out). This last conclusion is even stronger in the context of the present model, as lateral interactions now depend on a single optimized parameter; this indicates that even rather limited cell-cell signalling is sufficient for cluster resolution.

Investigation of our present model has also revealed that

variations in the strength of lateral signalling have a heterochronic effect on cluster resolution (Fig. 4). This may have some bearing upon issues such as the differences in bristle number between different fly species. Researchers have considered these differences as the result of altered patterns of expression of genes that set up proneural clusters (Simpson 1996). Our work suggests that variation in the strength of lateral signalling may also contribute to bristle number phenotypes.

Our optimization solutions have also been shown to be robust to small changes in initial conditions (Fig. 3). Of course one might argue that, since through our training dataset we look for solutions that result in the most central and most encircled cell of each cluster becoming the neural precursor, it is not surprising that with slightly different initial conditions the same cell is still selected. This is true, but the point is that, if in the biological system the same selection rule occurs, then our results show that this is a robust process. This point relates to questions raised in the literature about "lateral inhibition" versus "mutual inhibition" explanations of cluster resolution (see Introduction above). Our results would favor mutual inhibition as the most likely explanation, with position in cluster and degree of encirclement being the properties that shield the prospective neural precursor from inhibition from other cells.

Finally, perturbations of gene expression in individual cells in the model (Fig. 5) are a rich source of quantitative predictions about how cells would respond to externally imposed changes. Such predictions are now testable in *Drosophila* (Halfon *et al.* 1997).

In conclusion, the model described in this paper, sufficiently simple and faithful to experimental observations, can produce biologically intepretable results. With more quantitative data to optimize its parameters on and with experimental testing of its various predictions, it could become a good tool to probe the dynamics of developmental processes like neurogenesis.

Acknowledgements

We wish to thank Anne Bang, Chris Kintner and John Thomas for discussions, Jim Posakony for discussions and fly stocks, Terry Sejnowski for use of the confocal microscope in his lab, and Larry Carter (UCSD and SDSC) and the Yale Center for Parallel Supercomputing for use of their computers. This work was supported in part by Office of Naval Research grant N00014-97-1-0422.

References

Artavanis-Tsakonas, S.; Matsuno, K.; and Fortini, M. 1995. Notch signaling. *Science* 268:225–232.

Bailey, A., and Posakony, J. 1995. Suppressor of Hairless directly activates transcription of *Enhancer of split* complex genes in response to Notch receptor activity. *Genes and Development* 9:2609–2622.

Bang, A.; Bailey, A.; and Posakony, J. 1995. *Hairless* promotes stable commitment to the sensory organ precursor cell fate by negatively regulating the activity of the *Notch* signaling pathway. *Developmental Biology* 172:479–494.

Bate, C. 1976. Embryogenesis of an insect nervous system. I. A map of the thoracic and abdominal neuroblasts in *Locusta migratoria*. *Journal of Embryology and Experimental Morphology* 35:107–123.

Campuzano, S., and Modollel, J. 1992. Patterning of the *Drosophila* nervous system - the *achaete-scute* gene complex. *Trends in Genetics* 8:202–208.

Cubas, P.; de Celis, J.-F.; Campuzano, S.; and Modolell, J. 1991. Proneural clusters of *achaete-scute* expression and the generation of sensory organs in the *Drosophila* imaginal wing disc. *Genes and Development* 5:996–1008.

Doe, C., and Goodman, C. 1985a. Early events in insect neurogenesis. I. Development and segmental differences in the pattern of neuronal precursor cells. *Developmental Biology* 111:193–205.

Doe, C., and Goodman, C. 1985b. Early events in insect neurogenesis. II. The role of cell interactions and cell lineage in the determination of neuronal precursor cells. *Developmental Biology* 111:206–219.

Fehon, R.; Kooh, P.; Rebay, I.; Regan, C.; Xu, T.; Muskavitch, M.; and Artavanis-Tsakonas, S. 1990. Molecular interactions between the protein products of the neurogenic loci *Notch* and *Delta*, two EGF-homologous genes in *Drosophila*. *Cell* 61:523–534.

Fleischer, K., and Barr, A. 1994. A simulation testbed for the study of multicellular development: The multiple mechanisms of morphogenesis. In Langton, C., ed., *Artificial Life III : Proceedings of the Workshop on Artificial Life, held June 1992 in Santa Fe, New Mexico*. Reading, MA: Addison-Wesley.

Fleischer, K. 1995. *A Simulation Testbed for the Study of Multicellular Development: Multiple Mechanisms of Morphogenesis*. Ph.D. Dissertation, California Institute of Technology.

Fortini, M., and Artavanis-Tsakonas, S. 1994. The Suppressor of Hairless protein participates in Notch receptor signaling. *Cell* 79:273–282.

Goriely, A.; Dumont, N.; Dambly-Chaudière, C.; and Ghysen, A. 1991. The determination of sense organs in *Drosophila*: Effect of the neurogenic mutations in the embryo. *Development* 113:1395–1404.

Halfon, M.; Kose, H.; Chiba, A.; and Keshishian, H. 1997. Targeted gene expression without a tissue-specific promoter: Creating mosaic embryos using laser-induced single-cell heat shock. *Proceedings of the*

National Academy of Sciences USA 94:6255–6260.

Hartenstein, V., and Posakony, J. 1989. Development of the adult sensilla on the wing and notum of *Drosophila melanogaster*. *Development* 107:389–405.

Heitzler, P., and Simpson, P. 1991. The choice of cell fate in the epidermis of *Drosophila*. *Cell* 64:1083–1092.

Huang, F.; Dambly-Chaudière, C.; and Ghysen, A. 1991. The emergence of sensory organs in the wing disc of *Drosophila*. *Development* 111:1087–1095.

Jarriault, S.; Brou, C.; Logeat, F.; Schroeter, E.; Kopan, R.; and Israel, A. 1995. Signalling downstream of activated mammalian Notch. *Nature* 377:355–358.

Jennings, B.; Preiss, A.; Delidakis, C.; and Bray, S. 1994. The Notch signalling pathway is required for *Enhancer of split* bHLH protein expression during neurogenesis in the *Drosophila* embryo. *Development* 120:3537–3548.

Lehmann, R.; Jiménez, F.; Dietrich, U.; and Campos-Ortega, J. 1983. On the phenotype and development of mutants of early neurogenesis in *Drosophila melanogaster*. *Wilhelm Roux's Archives of Developmental Biology* 192:62–74.

Marnellos, G., and Mjolsness, E. 1998. A gene network approach to modeling early neurogenesis in Drosophila. In *Pacific Symposium on Biocomputing*, volume 3, 30–41.

Marnellos, G. 1997. *Gene Network Models Applied to Questions in Development and Evolution*. Ph.D. Dissertation, Yale University.

Martin-Bermudo, M.; Martinez, C.; Rodriguez, A.; and Jimenez, F. 1991. Distribution and function of the *lethal of scute* gene product during early neurogenesis in *Drosophila*. *Development* 113:445–454.

Mjolsness, E.; Sharp, D.; and Reinitz, J. 1991. A connectionist model of development. *Journal of Theoretical Biology* 152:429–453.

Muskavitch, M. 1994. Delta-Notch signalling and *Drosophila* cell fate choice. *Developmental Biology* 166:415–430.

Poulson, D. 1940. The effect of certain X-chromosome deficiencies on the embryonic development of *Drosophila melanogaster*. *Journal of Experimental Zoology* 83:271–318.

Romani, S.; Campuzano, S.; Macagno, E.; and J., M. 1989. Expression of *achaete* and *scute* genes in *Drosophila* imaginal discs and their function in sensory organ development. *Genes and Development* 3:997–1007.

Simpson, P. 1996. *Drosophila* development: A prepattern for sensory organs. *Current Biology* 6:948–950.

Skeath, J., and Carroll, S. 1991. Regulation of *achaete-scute* gene expression and sensory organ pattern formation in the *Drosophila* wing. *Genes and Development* 5:984–995.

Skeath, J., and Carroll, S. 1992. Regulation of proneural gene expression and cell fate during neuroblast segregation in the *Drosophila* embryo. *Development* 114:939–946.

Stern, C. 1954. Two or three bristles. *American Scientist* 42:213–247.

Struhl, G.; Fitzgerald, K.; and Greenwald, I. 1993. Intrinsic activity of the Lin-12 and Notch intracellular domains *in vivo*. *Cell* 74:331–345.

van Doren, M.; Powell, P.; Pasternak, D.; Singson, A.; and Posakony, J. 1992. Spatial regulation of proneural gene activity: Auto- and cross-activation of *achaete* is antagonized by *extramacrochaetae*. *Genes and Development* 6:2592–2605.

Wigglesworth, V, B. 1940. Local and general factors in the development of "pattern" in *Rhodnius prolixus*. *Journal of Experimental Zoology* 17:180–200.